Available online at www.sciencedirect.com
SCIENCE DIRECT®

Journal of Magnetism and Magnetic Materials 267 (2003) 111–114

journal of magnetism and magnetic materials

www.elsevier.com/locate/jmmm

Anomalous magnetic properties of antiferromagnetic CoO nanoparticles

Liying Zhang, Desheng Xue*, Cunxu Gao

Key Laboratory for Magnetism and Magnetic Materials of the Ministry of Education, Lanzhou University, Lanzhou 730000, People's Republic of China

Received 17 January 2003; received in revised form 4 April 2003

Abstract

Antiferromagnetic CoO nanoparticles ranging from 10 to 80 nm were prepared by the sol–gel process. The morphology, size and structure of the particle were characterized by TEM microscopy, electron diffraction and X-ray diffraction. Magnetic properties were measured using VSM and MPMS magnetometers. The nanoparticles has an FCC structure with a lattice parameter of 4.258 Å. Anomalous magnetic properties, such as hysteresis, were observed in CoO nanoparticles comparing to the course grain materials. The coercive force increases as the particle size is reduced, but decreases when the size is less than 20 nm. The magnetization increases below 100 K for the nanoparticles. However, no significant shifts of Neel temperature were observed. This magnetic behavior could be interpreted in terms of a core-shell model, in combination with the magnetic interaction between particles.

PACS: 75.50.Ee; 75.50.Tt; 75.60.Ej; 75.75.+a

Keywords: Antiferromagnetism; Nanoparticles; Magnetization curves; Hysteresis

1. Introduction

Magnetic properties of nano-sized particles are of great importance from basic as well as applications point of view [1,2]. Neel has originally pulled the attention to the properties of antiferromagnetic nanoparticles (AFN) in 1961 [3]. He suggested that small antiferromagnetic particles, due to the uncompensated number of spins on two sublattices, should exhibit superparamagnetism and weak ferromagnetism. In the following years the magnetic behavior was experimentally studied in some AFN, such as NiO [4–6], MnO [7] and hematite (α-Fe_2O_3) [8,9]. However, few works were reported on the magnetic properties of CoO nanoparticles whereas there are a few studies [10–13].

The mechanism that gives rise to the net moment of AFN is still a matter of investigation due to the complicated surface effects. Kodama et al. [4] suggested that the reduced coordination of the surface spins might result in a stabilization of multi-sublattice configurations with respect to the classical 2-sublattice one. However, Flipse et al.

*Corresponding author. Tel: +86-931-8912726; fax: +86-931-8912726.

E-mail addresses: xueds@lzu.edu.cn (D. Xue), liyingzhang@lzu.edu.cn (L. Zhang).

0304-8853/03/$ - see front matter
doi:10.1016/S0304-8853(03)00343-3

[11] observed a large orbital contribution to the magnetic moment at low temperature, which can cause a change in magnetic ordering in the core of the particles. In this paper, we report the preparation and magnetic properties of CoO nanoparticles. The magnetic behaviors observed on nanoparticles are interpreted in terms of a simple core-shell model, in combination with the magnetic interaction between particles.

2. Experimental

The preparation of CoO nanoparticles has been described in detail elsewhere [14]. A gel precursor powders can be obtained after drying the mixed solution, which consists of $Co(NO_3)_2 \cdot 6H_2O$ and polyvinylalcohol (PVA). CoO nanoparticles were synthesized by heat treating the gel powders at 225°C for 1 h in H_2. The mean size of the particles can be tuned by adjusting the concentration of the solution. A coarse grain powder was prepared by decomposing the cobalt nitrate at 1173 K for 1 h in air.

The morphology, size and structure of the sample were analyzed by a JEM-1200EX transmission electron microscope (TEM) and a Rigaku D/max-2400 X-ray diffractometer with Cu $K\alpha_1$ radiation. The magnetic properties of the sample at room temperature were performed on the Lake Shore 7304 vibrating sample magnetometer (VSM). The temperature dependence of the magnetization ($M-T$) for the sample was carried out using the commercial MPMS magnetometer.

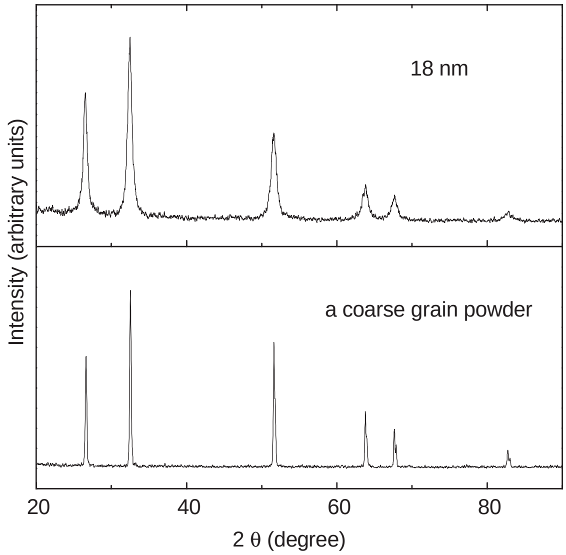

Fig. 1. XRD patterns of 18 nm CoO nanoparticles and a coarse grain powder.

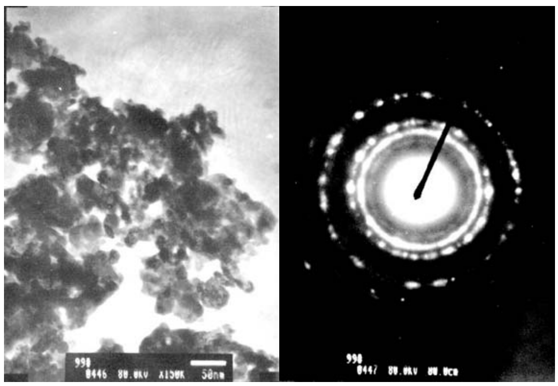

Fig. 2. TEM image and selected area electron diffraction pattern of 18 nm CoO nanoparticles.

3. Results and discussion

The representative X-ray diffraction (XRD) patterns of the CoO nanoparticles and the coarse grain powder are shown in Fig. 1. Both figures show an FCC structure with a lattice parameter of 4.258 Å, which is in well agreement with the bulk CoO materials (4.26 Å). The mean size of the nanoparticles calculated by using Scherrer's equation from broadening peaks was 18 nm. It is found that the size of particle in the range 10–80 nm can be prepared by tuning the concentration of solution.

Fig. 2 shows the typical TEM image and the selected electron diffraction patterns of the CoO nanoparticles. The mean size and structure is in agreement with the XRD results except for some agglomerated particles. The existence of these aggregates will increase the magnetic interaction between particles, and therefore maybe affect the magnetic properties of the CoO nanoparticles.

Fig. 3 shows the hysteresis loops of the CoO nanoparticles and the coarse grain powder. The linear-shape of the hysteresis loop of the coarse grain powder shows the characteristic of antiferromagnetism. However, an "S"-like shape of hysteresis loop was observed as the particle size was reduced to 80 nm, and the shape of the hysteresis loop evolves with the mean size of the particle. The shape of the hysteresis loops can be divided into two portions: a curvature and a linear, maybe corresponding to the ferromagnetic contribution and the antiferromagnetic or paramagnetic one, respectively. Considering our samples, which are the antiferromagnetic CoO nanoparticles, the ferromagnetic portion is attributed to the increase of the uncompensated moments at the disordered particle surface resulting from the reduced coordination of the surface spins [7–9,15], The linear one is mainly due to the antiferromagnetic structure of the particle core. This magnetic behavior seems to indicate that our sample can be described in terms of the simple core–shell model.

The size dependence of coercive force is shown in the inset of Fig. 3. It can be seen that the coercive force increases with decreasing size, but decreases when the size is less than about 20 nm. It can be easily understood that the number of uncompensated spins at the surface shell will increase as the particle size is reduced, and therefore the net magnetization will also increase, which can bring the increase of the coercive force. On the other hand, the static magnetic interaction between particles will increase with the increasing net magnetization, which can decrease the coercive force [7,16]. Furthermore, the effective magnetocrystalline anisotropy of the nanoparticle will decrease as the particle size is reduced, which will decrease the coercive force. In summary, the increase of coercive force with the decreasing size is mainly attributed to the increasing number of uncompensated spins at surface shell. The increased static magnetic interaction and reduced effective magnetocrystalline anisotropy are mainly responsible for the decrease of the coercive force when the particle size is less than 20 nm. Analogous results were also observed on NiO [4] and MnO [7] nanoparticles.

The typical $M-T$ curves of CoO nanoparticles and the coarse grain powder are shown in Fig. 4.

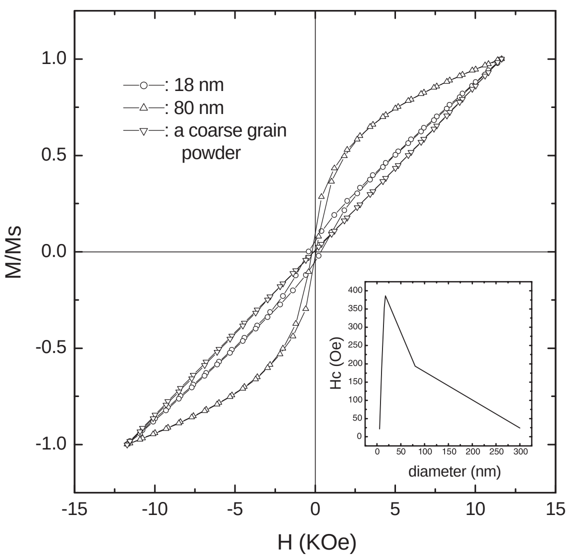

Fig. 3. Hysteresis loops of the coarse grain powder and the CoO nanoparticles with the size of 18 and 80 nm at room temperature. Inset is the coercive force as functions of the particle size.

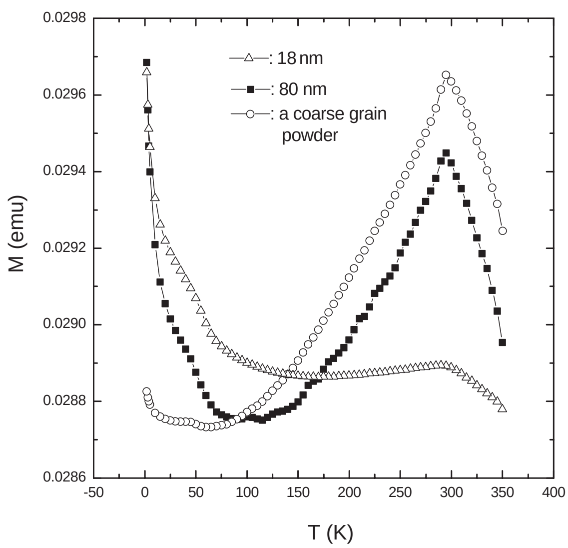

Fig. 4. The temperature dependence of magnetization curves of the coarse grain powder and the CoO nanoparticles with size of 18 and 80 nm from 1.9 to 350 K in magnetic field of 10 kOe.

The increase of the magnetization with the increasing temperature below Neel temperature (T_N) indicates the characteristic of antiferromagnetism. However, the intensity of magnetization peaks at the T_N decrease with the reduction of the particle size, and almost nondependent with the temperature at the range 100–293 K when the size is reduced to 18 nm. This indicates that the characteristic of antiferromagnetism is weakened gradually as the particle size is reduced. Simultaneously, the magnetization increases below 100 K for the nanoparticles, which indicates that the surface effect resulting from the increasing number of spins at the surface shell increases with the reduction of the particle size. That is to say, the attribution of the antiferromagnetism in the particle core decreases with the decrease of particle size, and that of the weak ferromagnetism at the surface shell increases correspondingly. However, unlike many other antiferromagnetic nano-materials, no significant shifts of T_N were observed in our experiments. This indicates that the surface effect is not strong enough to destroy the antiferromagnetic exchange coupling in the particle core.

4. Conclusion

Antiferromagnetic CoO nanoparticles ranging from 10 to 80 nm have been synthesized by using a sol–gel process. The nanoparticles has an FCC structure with a lattice parameter of 4.258 Å. Anomalous magnetic properties were observed in these particles and interpreted in terms of a core–shell model. The hysteresis is attributed to the switching of the uncompensated moments at the disordered particle surface shell. The size dependence of coercive force can be interpreted by the degree of the uncompensated moments, magnetic interaction between particles and the effective magnetocrystalline anisotropy. The increase of the magnetization below 100 K results from the increasing number of spins at the surface shell. No significant shifts of Neel temperature observed indicate that the surface effect is not strong enough to destroy the exchange coupling in the particle core.

Acknowledgements

The author is grateful to Dr. P.H. Zhou for measuring the magnetic properties on MPMS magnetometer. This work is supported by NSFC of China (Grant No 50171032).

References

[1] R.W. Chantrell, K. O'Grady, in: Applied Magnetism, Kluwer Academic, The Netherlands, 1994, p. 113.
[2] I.S. Jacobs, C.P. Bean, in: Magnetism, Vol. 3, Academic Press, New York, 1963, p. 294.
[3] L. Neel, Compt. Rend. 252 (1961) 4075.
[4] R.H. Kodama, S.A. Makhlouf, A.E. Berkowitz, Phys. Rev. Lett. 79 (1997) 1393.
[5] S.A. Makhlouf, F.T. Parker, F.E. Spada, A.E. Berkowitz, J. Appl. Phys. 81 (1997) 5561.
[6] F. Bødker, M.F. Hansen, C. bender Koch, S. Mørup, J. Magn. Magn. Mater. 221 (2000) 32.
[7] Sanshiro Sako, Yoshifumi Umemura, Kazunari Ohshima, Masahiro Sakai, J. Phys. Soc. Jpn. 65 (1995) 280.
[8] M.F. Hansen, F. Bødker, S. Mørup, K. Lefmann, K.N. Clausen, P.A. Lindgard, Phys. Rev. Lett. 79 (1997) 4910.
[9] F. Bødker, M.F. Hansen, C. bender Koch, K. Lefmann, S. Mørup, Phys. Rev. B 61 (2000) 6826.
[10] J.S. Yin, Z.L. Wang, Phys. Rev. Lett. 79 (1997) 2570.
[11] C.F.J. Flipse, C.B. Rouwelaar, F.M.F. de Groot, Eur. Phys. J. D. 9 (1999) 479.
[12] L. Soriano, M. Abbate, A. Fernández, A.R. Gonzáles-Elipe, F. Sirotte, J.M. Sanz, J. Phys. Chem. B 103 (1999) 6676.
[13] M. Verelst, T.O. Ely, C. Amiens, E. Snoeck, P. Lecante, A. Mosset, M. Respaud, J.M. Broto, B. Chaudret, Chem. Mater. 11 (1999) 2702.
[14] Liying Zhang, Desheng Xue, J. Mater. Sci. Lett. 21 (2002) 1931.
[15] C. Gilles, P. Bonville, H. Rakoto, J.M. Broto, K.K.W. Wong, S. Mann, J. Magn. Magn. Mater. 241 (2002) 430.
[16] R.D. Zysler, D. Fiorani, A.M. Testa, J. Magn. Magn. Mater. 224 (2001) 5.